Modelling Of Swirl Jet Flows

M. Meyyappan[1,2,3], M. P. Schwarz[1] and J. H. Perry[1,2]

1. CSIRO Division of Minerals, Institute of Minerals Energy and Construction, Clayton, Victoria
2. CRC - New Technologies For Power Generation From Low-Rank Coal, Mulgrave, Victoria
3. Swinburne University of Technology, Hawthorn, Victoria

ABSTRACT

Different aspects of accurately modelling a swirl flow have been analysed. It has been shown that inclusion of upstream history in modelling has improved the prediction of recirculating flow patterns in a swirl jet to a greater accuracy. In addition a range of solution techniques to improve the predictions of swirling flows was identified such as applying Reynolds stress turbulence model whenever possible, utilising higher order differencing schemes and employing orthogonal co-ordinates.

1. INTRODUCTION

Flame stability is one of the prime concerns in the operation of a gas turbine combustor and it critically depends on the type of flow pattern in the primary zone, where the combustion takes place. Establishment of a flow pattern which creates a toroidal flow reversal, entraining and recirculating the hot combustion products to mix with incoming air and fuel, is highly desirable. Prediction of such a flow pattern is a very challenging exercise since the developed recirculating flow pattern is the result of a multitude of complex processes involving strong shear regions, high turbulence and rapid mixing rates. In this work various aspects of modelling swirl flows were analysed using the CFD code CFX-F3D (AEA Technology, 1995).

2. MODELLING

CFX-F3D is a general purpose 3-D finite difference CFD code. It uses a non-staggered grid, with the Rhie-Chow algorithm used to prevent oscillations in the pressure field. For incompressible flows, the code uses the Reynold's time averaging for the fluctuating turbulent quantities.

The governing equations of mass and momentum for a steady state and incompressible flow are defined (see Shore et al., 1995) using the Navier Stokes equations. The velocity-pressure coupling has been effected through the SIMPLEC algorithm (Van Doormal and Raithby, 1984) which provides the basis for updating pressure and correcting velocity components for continuity.

Of the different turbulence models available, two widely used turbulence schemes: k-ε turbulence model which uses eddy viscosity hypothesis and Reynolds stress turbulence model which employs additional transport equations solving individual components of the Reynolds stress, are utilised in this work. Since these two schemes are well known and widely published, the mathematical details are not provided here.

2.1. Experimental Data

The experimental data published by Charles and Samuelson (1988) for the gaseous combustion of an axisymmetric can type gas combustor was selected for validating the results of different numerical approaches. The combustor consists of a cylindrical stainless steel tube, with swirl vanes (imparting 60^{o} turn to the flow) concentrically located within the tube around a centrally positioned fuel delivery tube. Gaseous propane fuel is introduced through a cone annular nozzle at the end of the central fuel delivery tube.

2.2. Upstream Modelling

In validating the code against the physical model of Charles and Samuelson (1988), the upstream history of secondary swirling air stream was included to create a model referred to here as

Upstream model (figure 1) using cylindrical co-ordinates. Symmetric flow field facilitated modelling of just a segment of the cylinder, housing a swirl vane at its centre, and assuming periodic boundary conditions at either end of the cylindrical segment. The flow geometry was split into three sections *Upstream, Swirler* and *Combustion chamber.* The *Upstream* section models the flow from the delivery pipe to the inlet of the swirl vanes. The *Swirler* section models the flow past the swirl vanes. This section is tilted by 60^{0} in order to turn the flow. The *Combustion chamber* models the flow from the swirl vanes to the end of the combustion chamber.

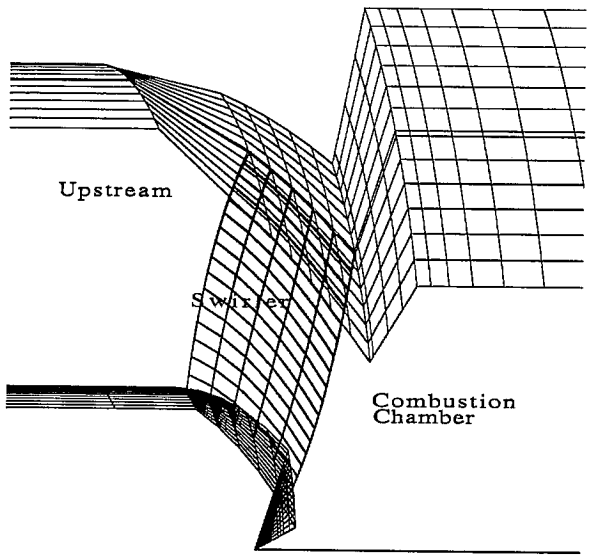

Fig 1. Upstream model geometry

Turbulence was modelled using the k - ε scheme owing to acute convergence difficulties experienced with the Reynolds stress model. The *hybrid differencing* scheme was used for solving the momentum and energy equations. Convergence was based on tolerance on mass source residual, sum of the absolute values of the net mass fluxes into or out of every cell in the flow. Since the overall aim is to refine the modelling techniques as applied to realistic and practical geometries, a relatively coarse grid which is finer near the burner outlet plane and the walls was used.

2.3. Comparison with a No-Upstream Model

Ignoring the upstream history of the swirling secondary flow and limiting the simulation to the combustor leads to models referred to here as 'No-upstream' models. Since the prediction of the aerodynamic field is very sensitive to the variations in inlet flow and physical boundary conditions (Charles et al., 1987), it is imperative to meticulously model the inlet boundary conditions. In 'No-upstream' models since the upstream history is ignored it becomes essential to set inlet boundary conditions at the burner outlet plane accurately in order to reproduce recirculating flow patterns. However accurate inlet boundary conditions at the burner outlet plane are seldom measured or documented under combustion conditions.

Hence for 'No-upstream' models, inlet boundary conditions at the burner outlet plane are specified by mean values of axial and swirl velocity components. The profile of radial velocity, which though smaller in magnitude can be crucial to the development of swirl flow, is hard to evaluate unless physically measured and hence could not be set at the inlet. As in 'Upstream' model, the k--ε turbulence model was employed along with the *hybrid* differencing scheme. Figure 2 compares recirculations predicted with 'No-upstream' model with that of the 'Upstream' model. In the 'Upstream' model simulation was extended to include the upstream history, modelling the development of flow in the secondary stream. The computational details of the 'Upstream' model are explained later.

In the experimental results a strong recirculation is observed closer to the swirling secondary stream inlet to the combustor. Recirculation is almost absent in the prediction of 'No-upstream' model, except near the fuel injector; by comparison, the 'Upstream' model predicted a well developed recirculation. However the recirculation lies closer to the combustor's axis and is relatively weaker compared to the physical measurements. This result can be improved as explained later and at this stage it suffices to emphasis the significance of upstream modelling and the difference it can make in accurately reproducing the recirculations.

The importance of accurate representation of the geometry and inlet conditions was also stressed by Cho and Fletcher (1991) who found that accurate specification of inlet length scale and radial velocity profile is essential to predict

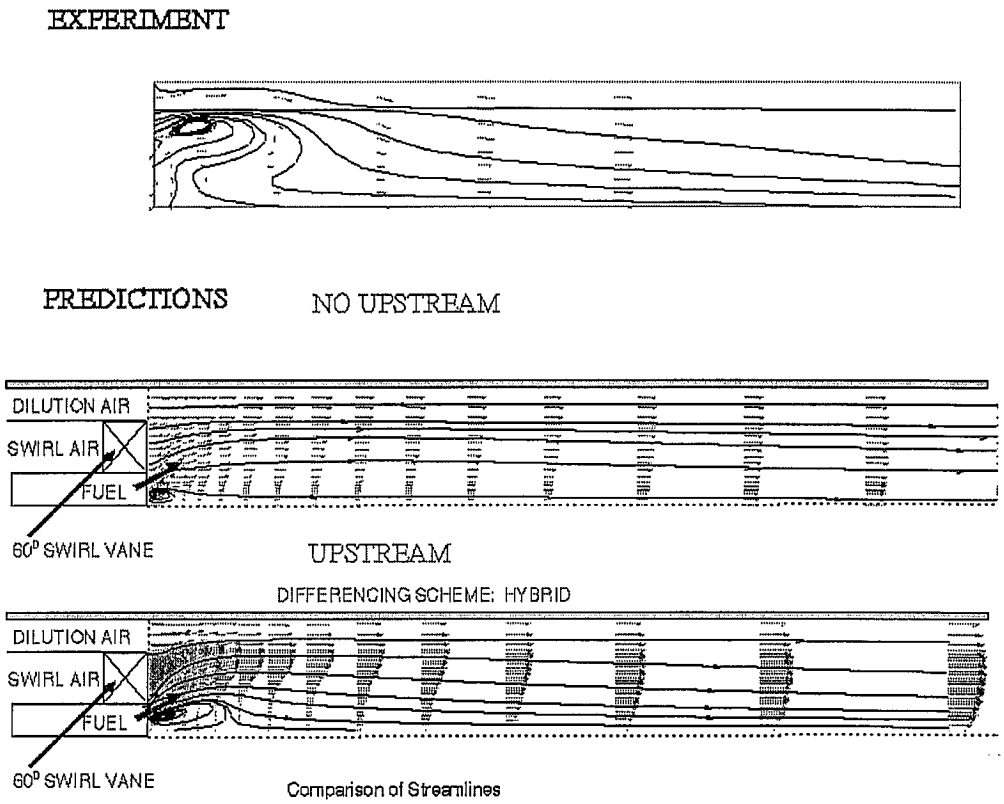

Fig 2. Comparison of 'No-upstream' & 'Upstream' predictions.

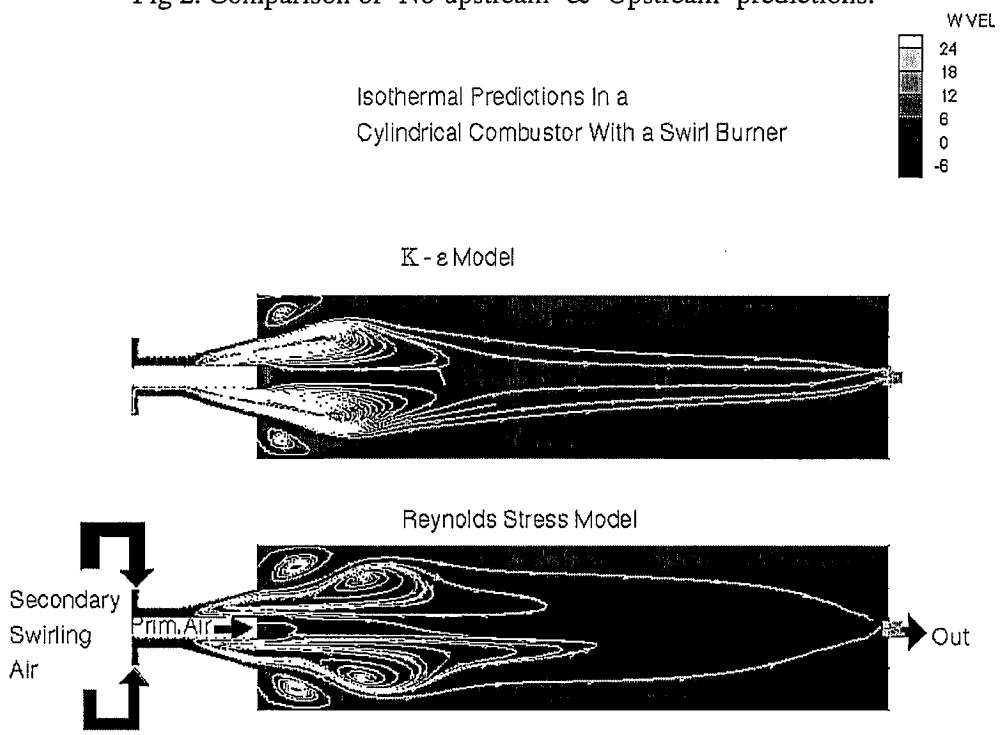

Fig 3. Different turbulence schemes - comparison.

correct axial decay of k and mean axial velocity in a conical diffuser flow. The dependence of solution accuracy on the specification of inlet length scale values was also observed for a highly swirling flow (Hogg and Leschnizer, 1989).

3. TURBULENCE MODELS

In applications of these types, two popular turbulence models, namely, the k- ε and the *Reynolds stress* models are generally applied to predict flow field. While the k- ε model is computationally inexpensive and free of any convergence problems, its assumption of isotropic diffusion limits its ability to accurately simulate the highly anisotropic swirling flow. The computationally expensive *Reynolds stress* model, which does not suffer from this disadvantage is generally expected to produce more accurate results but it is known to subject to convergence difficulties especially when applied for a complex geometry.

Owing to convergence difficulties, it was decided to evaluate the turbulence models in a different geometry based on the experimental results of Smith et al.(1989) from the ACIRL pilot- scale test furnace, a refractory lined vertical cylinder 0.66m in diameter and 2.5m long, down fired by a double concentric swirl burner. Swirl in the secondary stream is generated using an adjustable moving block swirl generator. Both the schemes were tried under isothermal conditions and the predicted mean axial velocities along with streamlines are given in the figure 3 where the dark shaded region represents the recirculation. From the figure it is obvious that the Reynolds stress scheme which accounts the anisotropic nature of the turbulence, predicts a stronger internal recirculation that extends to roughly half of the combustor and external recirculation closer to the combustor wall in the primary zone and appears to a better computational tool. Measurements were not carried out and hence a comparison could not be made with the physical model.

The Algebraic stress model, a simplified version of the Reynolds stress model where the Reynolds stress transport equations are replaced by algebraic equations, can also be considered. Cho and Fletcher (1991) used it successfully to predict mean flow and turbulence in complex turbulent flows with adverse axial pressure gradients and near-separation flow conditions.

4. DIFFERENCING SCHEMES

With the k - ε model defining the turbulence, different differencing schemes, ie., *Higher Upwind*, *QUICK* along with the general *hybrid* schemes, were tried mainly with the momentum equations. Higher order differencing schemes are more accurate but less robust and computationally expensive. The *Higher Upwind* scheme is a second order accurate upwind differencing scheme and can be regarded as a natural extension of the first order *upwind differencing* method. In this scheme mid-point values are found by extrapolating from the two points on the upwind side of the cell face under consideration. The *QUICK* scheme is a third order accurate upstream differencing scheme and it involves fitting a quadratic equation through three nodes (two on the upstream side and one on the downstream side of the cell face) and then using this equation to find mid-point values. Of these two schemes, *QUICK* has a tendency to diverge and needs to be under relaxed at the initial stages. No such trouble was observed with *Higher Upwind* scheme.

Predicted recirculation patterns are compared with experiment in figure 4. Experimental results indicate a strong swirling flow with the eye of recirculation located across the swirler outlet plane and the recirculation extending up to the combustor walls. Both higher order differencing schemes predicted flow patterns that are comparable in the length and shape but lie closer to the axis indicating a relatively weaker swirl. It can be safely inferred that higher order differencing schemes predicted to a greater accuracy than the *hybrid differencing* scheme and amongst the higher order differencing schemes, the *QUICK* scheme predicted marginally better recirculation that extends up to the dilution air stream.

The predictions of mean axial velocity are analysed in detail using the line plots drawn at different axial planes (figure 5). At an axial distance of X = 2 cm, very close to the burner outlet plane, experimental data indicates a strong reverse flow occurring roughly across the secondary stream inlet to the combustor with a peak in the positive mean axial velocity occurring closer to the wall of the combustor.

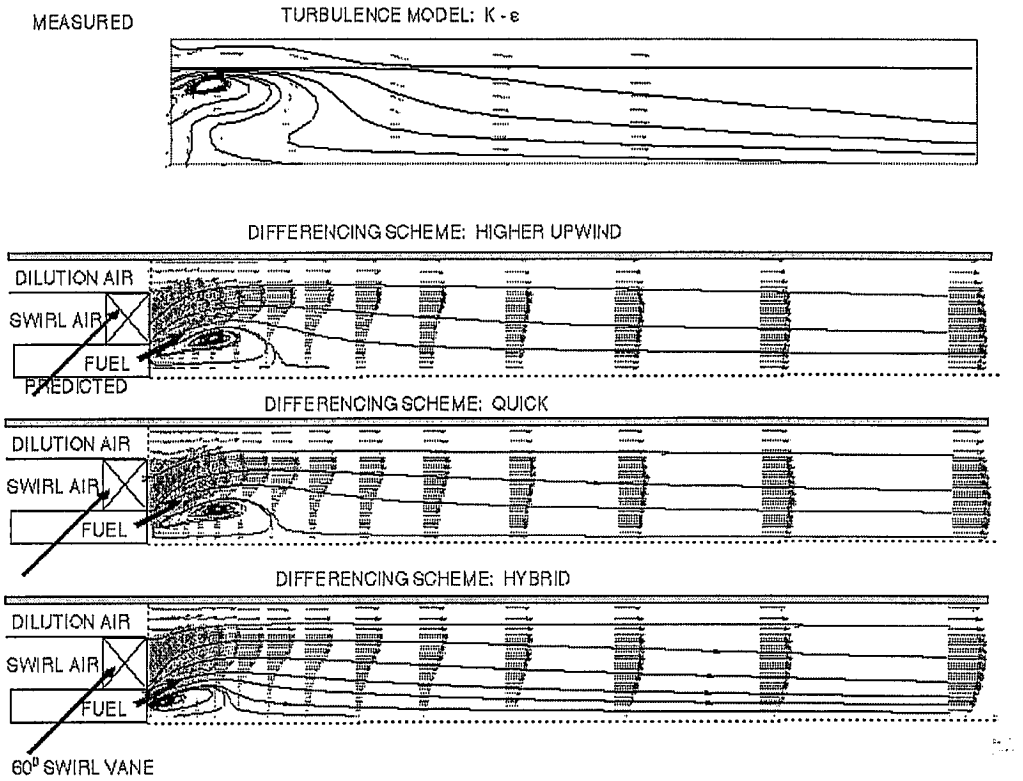

Fig 4. Different differencing schemes - comparison of streamlines predicted.

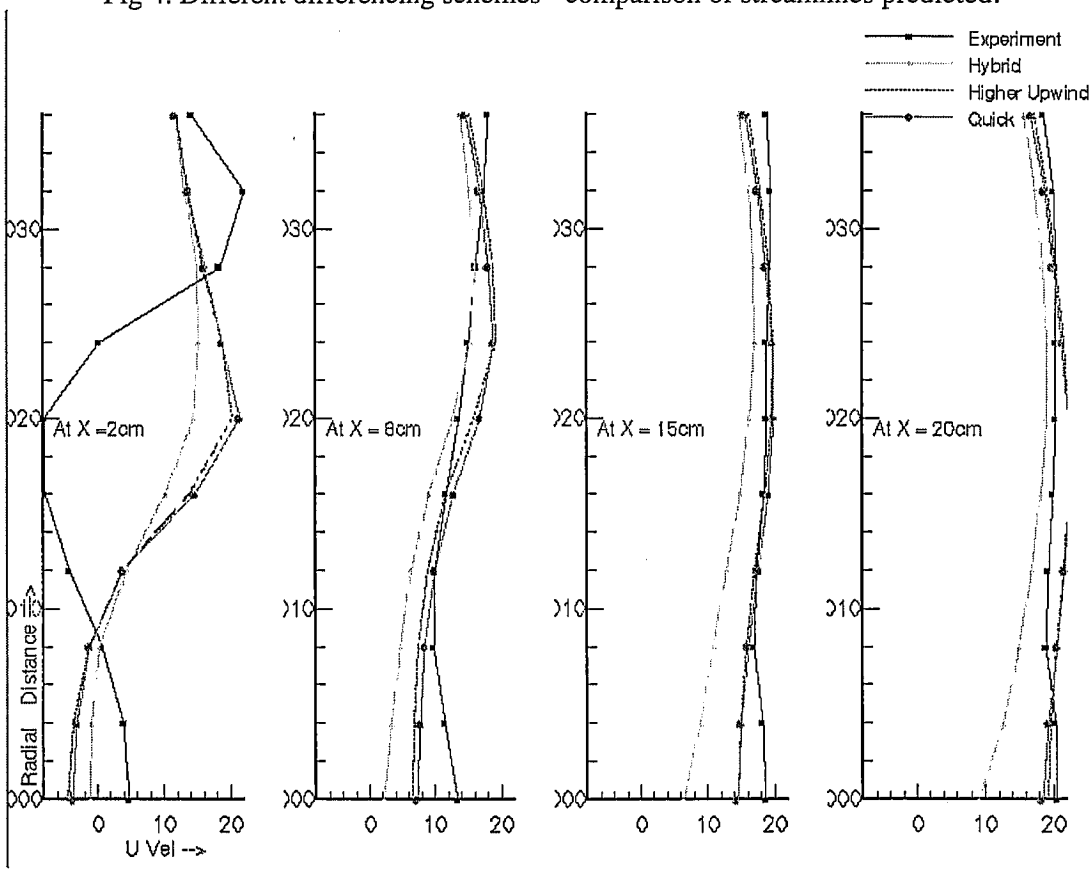

Fig 5. Different differencing schemes - comparison of mean axial velocities predicted.

Higher order differencing schemes predicted nearly equal peaks in the axial velocity but these maximum values occur roughly half way between the axis and the wall. The *hybrid* scheme predicted a flow pattern which is similar but weaker compared to the higher order schemes. With the predictions, reverse flow occur along the axis as discussed earlier. These discrepancies in the flow field between the physical measurements and the numerical model gradually disappears at planes farther away (X = 8,16 & 24 cm) from the burner outlet plane. The *hybrid* scheme however consistently under predicted the axial velocity.

Given the importance of accurately defining inlet boundary conditions, it proved to be a handicap not to have the actual geometry of the swirl vanes. A finer mesh at the swirler section can yield a better solution which however could not be tried due to convergence difficulties. It is worth noting the views of Smith et al. (1989) on the deficiency of all current turbulence models in predictingswirling flows. They observed that an artificial increase of the swirl number in primary zone produced results which matched with experimental data. Both the k- ε model and the Reynolds stress model use the dissipation rate equation which was derived through the Navier-Stokes equations for fluctuating vorticity and consists unknown complex correlations. Evaluation of correlations necessitated drastic model assumptions that are not universal (Rodi, 1984). Thus application of the ε equation lead to some loss of accuracy in the solution and particularly in the length scales predicted (Cho and Fletcher, 1991).

5. CO-ORDINATE SYSTEMS

Shore et al., (1995) studied the influence of orthogonal and non-orthogonal meshes in predicting a swirl flow along a cylindrical pipe. With an orthogonal grid they predicted better results that are sensitive to the type of turbulence schemes but insensitive to the choice of convection scheme. In the non-orthogonal grid, the choice of convection scheme played a crucial role. These interesting numerical findings were however not validated by comparisons with experiment and their work confined to simple geometry and velocities which are not very high. These issues are addressed in this section.

Musgrove and Hooper (1993) measured the swirling flow field generated in a 6m long pipe of internal diameter 142 mm. The swirling was effected by a single start Archimedean spiral of 5 turns with a pitch to diameter ratio of 1.52 which forms the annulus of a 50 mm diameter inner pipe located near the exit of the 6m long pipe. The last turn of the spiral projected past the end of the pipe 75 mm to ensure a complicated asymmetric jet.

5.1. Numerical Modelling

The significance of upstream modelling is accentuated further with this modelling since a decision to ignore the upstream history will lead to setting up of unrealistic boundary conditions at the swirler outlet, with one third of the spiral's last turn projected. Hence a model geometry was constructed which includes the upstream flow field starting from entrance of the 6m long pipe. The orthogonal grid was constructed using cylindrical co-ordinates and the non-orthogonal grid using Cartesian co-ordinates.

The model geometry of single start Archimedean spiral is shown in figure 6. For the non-orthogonal grid, the spiral section was constructed using a total of 600 blocks, with each 15° turn of the spiral modelled by a set of blocks. By comparison the orthogonal grid needed far fewer blocks. The spiral itself was modelled using thin surface patches which assume walls of zero thickness. As one would expect, the complex geometry and the high velocity flow (up to 140 m/s) in the spiral section lead to acute convergence difficulties especially as the flow was modelled using the Reynolds stress turbulence scheme. In contrast to the observation of Shore et al., (1995), it is the orthogonal grid where the convergence was difficult to achieve, owing to higher flow velocities. In the non-orthogonal grid the presence of numerical diffusion affects the accuracy of the solution developed leading to

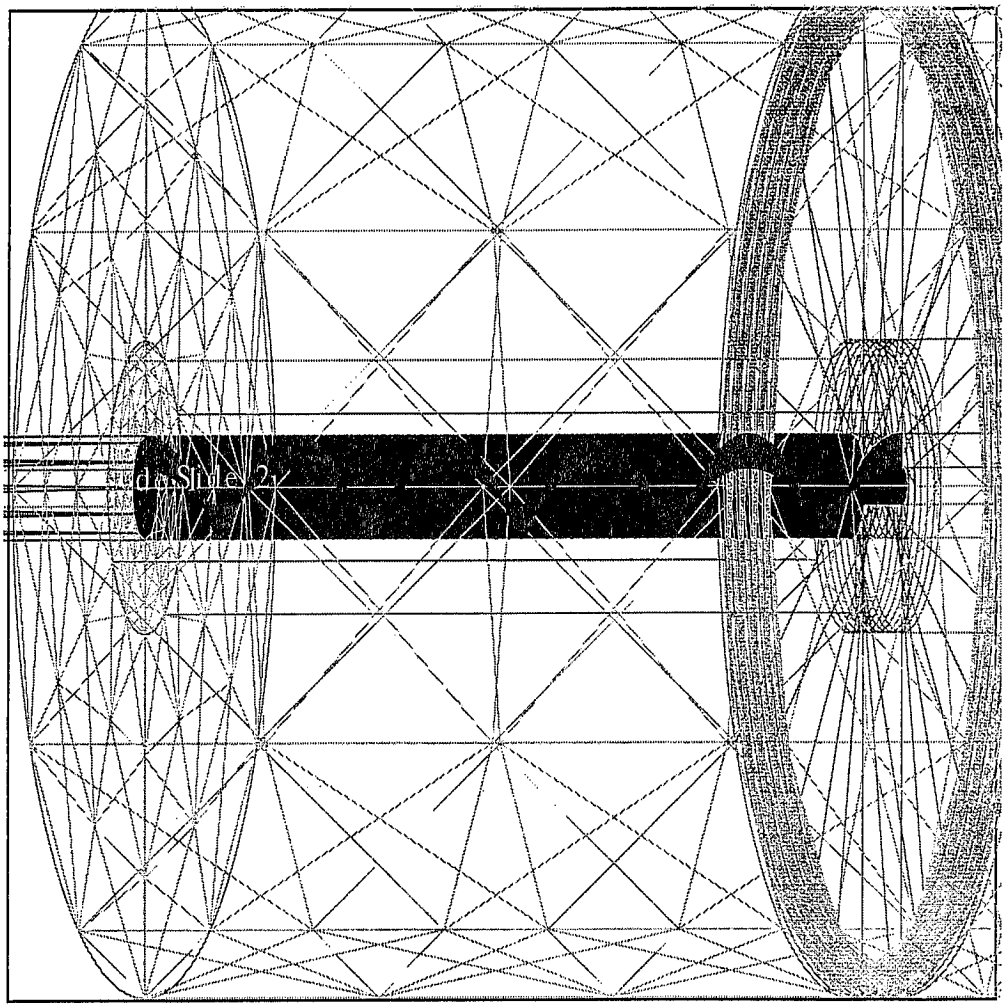

Fig 6. Computational model geometry showing details of spiral section.

predictions of rapid decay of the high velocity jets which however results in reduced velocities,apparently helping to stabilise the solution. Owing to the convergence difficulties higher order differencing schemes could not be used and the *hybrid scheme* was adopted instead.

5.2. Results and Discussions

The predicted mean axial velocity (normalised by 100 m/s) contours near the swirler outlet plane are compared with the experiment in figure 7, where *D* refers to the diameter of the outer tube. In the figure, the dark shaded region represents the flow in the reverse direction. The asymmetry of the flow field is reflected in a peak value of approximately 35 m/s of the forward jet in the upper half compared to a maximum value of 70 m/s in the lower half (of the flow domain) and in the observed location of the maximum reverse flow velocity, offset radially upwards. This recirculation appears to extend all the way up to the lower half of the outer pipe housing the spiral, and this can possibly explain the increased deflection of the lower forward jet away from the axis (around 23 - 25°) compared to that of the upper forward jet (around 12°).

With cylindrical co-ordinates the numerical model predicts the deflection of the lower forward jet to be around 20° and that of the upper jet to be around 15°, matching the experiment qualitatively and quantitatively within a reasonable accuracy. However the same cannot be said about the predictions using body-fitted co-ordinates which predicts the upper jet to deflect more (around 33°) compared to the lower jet (around 13°).

Analysing the magnitudes of the jets, the cylindrical co-ordinates predicts a maximum

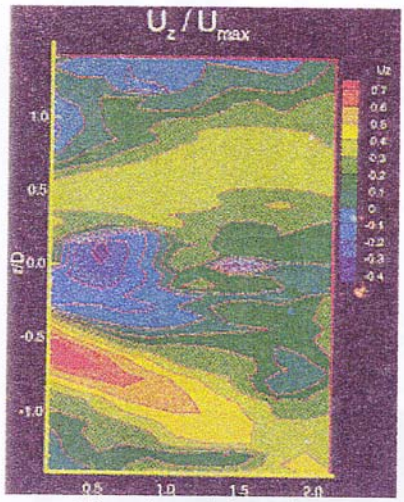

Experimental results

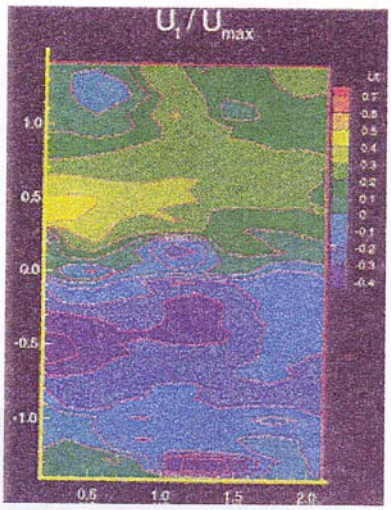

Experimental results

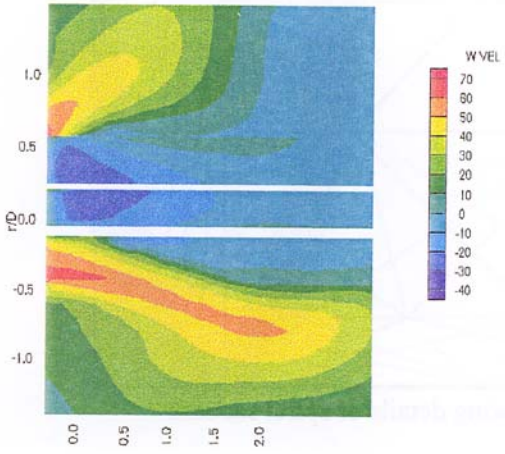

Predictions using non-orthogonal grid

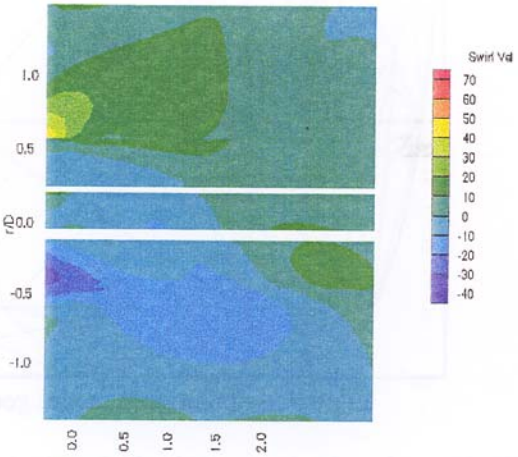

Predictions using non-orthogonal grid

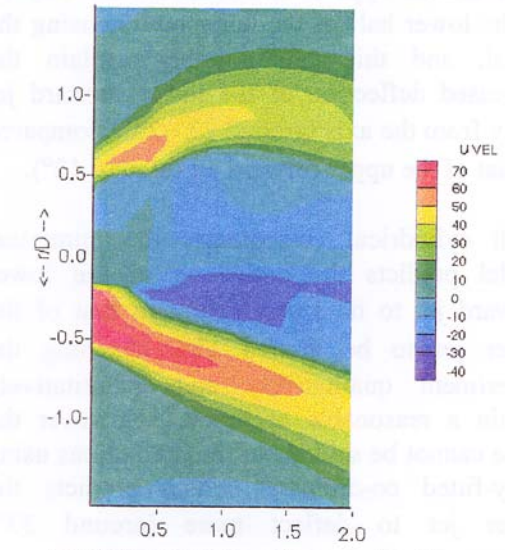

Predictions using orthogonal grid

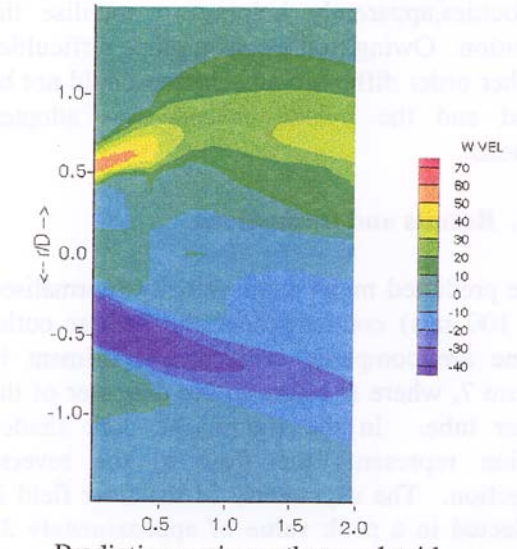

Predictions using orthogonal grid

Fig 7. Comparison of predicted mean axial velocity contours with experiment.

Fig 8. Comparison of predicted mean swirl velocity contours with experiment.

forward velocity of 70 m/s at the lower jet which agrees with the experiment, and a maximum forward velocity of around 55 m/s at the upper jet which is higher than the experimentally observed value. The corresponding peak values observed with the body-fitted co-ordinates are 70 m/s in the lower jet (as with experiment) and roughly 60 m/s in the upper jet. Both the co-ordinates systems predict recirculations that stay closer to the swirler outlet plane but extend over larger areas compared to the experiment.

Figure 8 compares the predicted mean swirl velocities with the experiment. High swirl velocities (40 m/s) are observed near the walls of the outer tube (at -0.5 and 0.5 r/D values) and the swirl velocities appear to be nearly symmetric where the high velocities occur, though the symmetry is lost closer to the axis. The orthogonal grid predicts a nearly matching swirl velocity profile with a maximum swirl velocity of around 50 m/s which is slightly higher than the experimentally observed value. It also predicts a nearly symmetric swirl flow field. Though the non-orthogonal grid predicts a maximum swirl velocity of around 45 m/s, closer to the experiment, the swirl momentum appears to dissipate rapidly along the axial direction and the near symmetry in the swirl flow observed experimentally and through the predictions with the orthogonal grid, appears to be lost.

A more detailed comparison is made using line plots generated in a radial plane closer to the swirler outlet plane where most of the prediction schemes are generally observed to be deficient. Figure 9 compares the mean normalised axial velocities predicted with experiment at a radial plane 25 mm downstream from the swirler outlet plane. Experimental results represented by square points reach a maximum value of 0.56 at a r/D value of -0.5, which physically corresponds to the lower wall of the outer tube. At the axis the mean axial velocity profile drops down to -0.08 indicating a reverse flow before peaking up to around 0.25 across the upper wall of the outer tube. The orthogonal grid predicts the peak at the lower jet to a good accuracy yielding a maximum value of 0.58 which compares well with the experimentally observed value of 0.56.

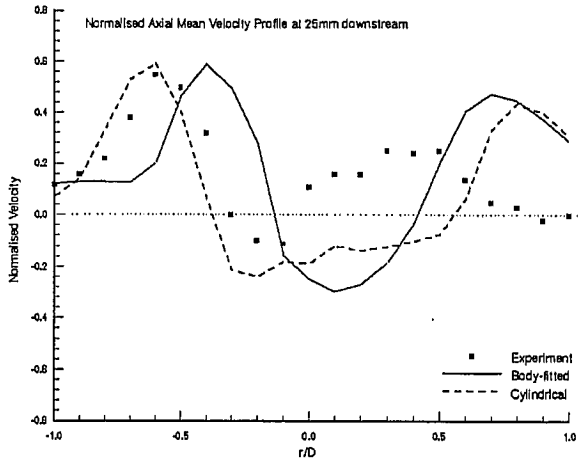

Fig 9. Comparison of predicted mean axial velocity profiles at 25 mm downstream from the swirl outlet plane.

At the upper half, the orthogonal grid predicts an extended recirculation and a higher maximum value (around 0.4) of the mean axial velocity. The non-orthogonal grid predicts a maximum (around 0.4) in the lower half, which is comparable to the experiment in magnitude, but differs in the location in that it occurs closer to the axis rather than at the lower tip of the outer tube. It predicts a stronger recirculation compared to the experiment and the orthogonal grid, at the axis before peaking to higher values in the upper half of the flow field.

Figure 10 compares the predicted normalised mean swirl velocity profiles at 25 mm downstream from the swirl outlet plane with experiment. The experimental profile is characterised with a maximum value of around 0.36 roughly across the lower tip of the outer pipe, a slight dip at the axis followed by a small increase and a final sharp dip to around -0.3 across the upper tip of the outer pipe. The orthogonal grid matches the lower half profile reasonably well by predicting a maximum (around 0.36), the dip and the subsequent rise at the axis. At the upper half it predicts a minimum value of around -0.22 which occurs above the upper tip of the outer pipe. The non-orthogonal grid predicts a comparable maximum value in the lower half though the profile differs in general with experiment and it also fails to pick up the dip and the subsequent rise at the axis. In the upper half it performs

reasonably well with a prediction of a minimum of around -0.2.

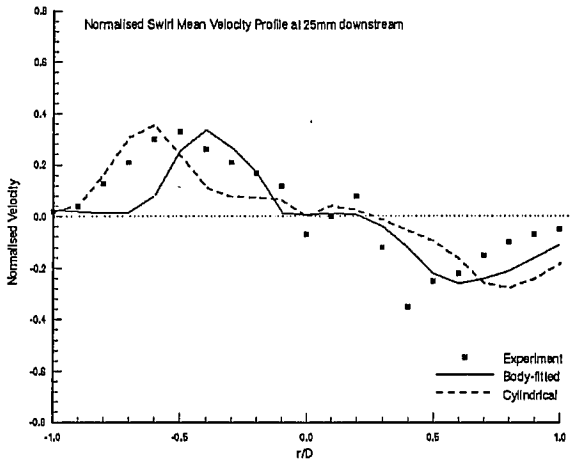

Fig 10. Comparison of predicted mean swirl velocity profiles at 25 mm downstream from the swirl outlet plane.

To summarise the influence of the grid structure in a complex geometry with higher flow velocities has been investigated. Owing to higher flow velocities the convergence was relatively difficult to achieve in the orthogonal grid. The orthogonal grid predicted the deflection of the forward jets qualitatively and quantitatively within a reasonable accuracy. The non-orthogonal grid predicted the upper jet to deflect more. Both the co-ordinates systems predicted recirculations that stay closer to the swirler outlet plane but extend over larger areas compared to the experiment, leading to predictions of higher axial velocities in the upper half of the flow field. The swirl velocity was better predicted by the orthogonal grid.

6. CONCLUSIONS

The significance of including upstream history in the modelling has been demonstrated with the 'Upstream' model reproducing the recirculating flow patterns to a greater accuracy. Of the two turbulence models, for complex geometry, the k-ε model proved to be an attractive option in terms of computational economy and ease of convergence. However the Reynolds stress scheme, which accounts for the anisotropic nature of the turbulence, predicted stronger internal recirculation in the jet flows investigated and appears to be a better computational tool. Of the different differencing schemes, predictions using the higher order differencing schemes the *Higher Upwind* and the *QUICK* were remarkably better than the *hybrid* scheme. Among the two higher order differencing schemes, the *QUICK* scheme's predictions were slightly better than the *Higher Upwind* scheme as far as the predictions of recirculating flow patterns are concerned.

An attempt has been made to test the influence of the grid structure by modelling a flow in a complex geometry with higher flow velocities using orthogonal and non-orthogonal grids and validate the results with an experimental data. Despite the convergence difficulties posed by the complex geometry and higher flow velocities, the orthogonal grid predicted flow field qualitatively and quantitatively within a reasonable accuracy.

ACKNOWLEDGEMENTS

The authors wish to acknowledge the support for this work by the Cooperative Research Centre for New Technologies For Power Generation From Low Rank Coal which is funded in part by the Cooperative Research Centres Program of the Commonwealth of Australia and CSIRO Division of Minerals - Clayton.

REFERENCES

AEA Technology, 1994, CFX-F3D, User Guide, Release 3.3., AEA Technology, Harwell Laboratory, Oxfordshire, UK.

Charles R.E., Brouwer J., and Samuelson G.S., 1987. The sensitivity of Swirl-Stabilised Distributed reactions to Inlet Flow and Physical Boundary Conditions, Presented at the *AIAA 25th Aerospace Sciences Meeting*, AIAA-87-0304.

Charles R.E., and Samuelson G.S., 1988, An Experimental Data Base for the Computational Fluid Dynamics of Combustors, *ASME* 88-GT-25.

Cho, N-H., Fletcher, C. A. J., 1991. Computation of Turbulent Conical Diffuser Flows using a Non-orthogonal Grid System,

Computers and Fluids, Vol. **10**, No. 3/4, 347-361.

Hogg, S. and Leschnizer, M. A., 1989. Computation of Highly swirling Confined Flow with a Reynolds Stress Turbulence Model, *AIAA J.* **27**, 57.

Musgrove, A. R. de L., and Hooper, J. D., 1993. Pressure Probe Measurements of the Turbulent Stress Distribution in a Swirling Jet, *Experimental Heat Transfer, Fluid Mechanics and Thermodynamics, M. D. Kelleher et al. (Editors), 1993 Elsevier Science Publishers B. V.*

Rodi, W., 1984. Turbulence Models and Their Application in Hydraulics, IAHR – Section on Fundamentals of Division II: Experimental and Mathematical Fluid Dynamics.

Shore, N. A., Haynes, B. S., Fletcher, D. F., and Sola, A. A., 1995. Numerical Aspects of Swirl Flow Computation, *Proceedings of the Seventh Biennial Conference, Computational Techniques and Applications: CTAC95*, Editors: Robert L. May and Alan K. Easton, World Scientific Publishing Co., 1996.

Smith I.W., Wall T.F., Baker J.W., Holcombe D., Harris D.J., Juniper L.A. and Truelove J.S., 1989. The Combustion Behaviour of Low-Volatile Australian Coals, *NERDDC Project 1110, End of Grant Report*, November 1989.

Van Doormal, J.P. and Raithby, G.D., 1984. Enhancements of the SIMPLE Method for Predicting Incompressible Fluid Flows, *Numerical Heat Transfer*, **7**, 147-163.